Aquilion Precision Ultra-High Resolution CT: Quantifying diagnostic image quality

Kirsten Boedeker, PhD, DABR
Senior Manager, Quantitative Image Quality
Canon Medical Systems Corporation

Introduction

Over the last thirty years, technological innovations have provided CT scanners with a continuous cycle of improvement to spatial and temporal resolution as well as overall faster scan times with wider anatomical coverage. Each technological advancement has provided clinicians the ability to expand the role of CT in the diagnosis of a wide array of clinical presentations. In addition, recent advances in detector and reconstruction technology have seen the radiation doses for a CT examination drop well below published industry-standard Dose Reference Levels (DRLs). Today, the Aquilion Precision ultra-high resolution CT system is making the power of routine, ultra-high resolution imaging — within industry-standard DRLs — a reality.

The ability to provide more accurate diagnosis through improved image quality is at the heart of every advance in imaging technology. The Aquilion Precision, making routine use of a ultra-high resolution detector, ultra-high resolution optics assembly, and ultra-high resolution 1024 matrix reconstruction, allows for visualization of fine detail to better delineate anatomical and pathological structures. As with any major innovation, a physics-based performance evaluation is critical to understanding and optimizing the Precision's ultra-high resolution modes in clinical use. Quantifying performance on high resolution images, especially relative to a conventional resolution system generally displayed on a 512 image matrix, requires a careful understanding of image quality metrics. Simple image quality measures, such as standard deviation and contrast-to-noise ratio, which do not include the effects of properties such as image texture and signal power, can be misleading, particularly as they relate to radiation dose. Consequently, the additional application of advanced image quality metrics is key to fully characterizing the Aquilion Precision. As such, the technical characteristics of the Aquilion Precision and methods for quantification of its associated image quality performance will be presented.

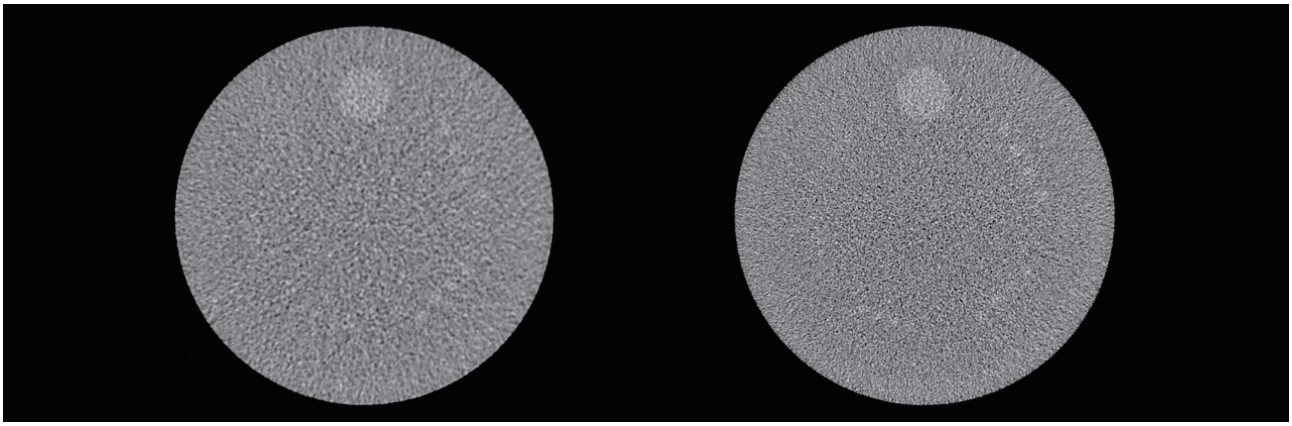

Figure 1 The HR mode image on the right has a lower CNR value than the NR mode image on the left, despite the HR mode image having superior visual low contrast detectability, illustrating the limitation of CNR as a measure of image quality.

The Aquilion Precision: A technical overview

Computed Tomography (CT) has always offered the image quality advantage of cross sectional imaging, unencumbered by anatomical overlap, as well as multi-planar reformats (MPRs) that allow the clinician to view anatomy in any plane. However, conventional CT lacks the in-plane high spatial resolution capabilities of routine Digital Radiography and MPRs are constrained by the resolving capability of the 0.5 mm or greater detector channel thickness. These constraints limit the visualization of fine detail, such as small vessels and airways, lung parenchyma, stent structure, and small tumors, as well as can lead to artifacts, such as blooming, and diminished ability to precisely quantify features of anatomical and pathological structures. As shown in Figure 2, the Aquilion Precision ultra-high resolution CT system offers in-plane spatial resolution of up to 150 µm × 150 µm, similar to Digital Radiography. In the longitudinal dimension resolution of up to 200 µm is achievable.

Ultra-high resolution, dose efficient imaging on the Aquilion Precision starts with its 0.25 mm × 160 row detector. The invention of proprietary cutting techniques has led to discrete detector elements that can be optically isolated, allowing for ultra-thin septa, resulting in a substantial increase in light-sensitive area on each element (Figure 3). This advancement, coupled with innovations in scintillator efficiency, detector circuitry and other DAS components, has led to the most dose efficient detector in company history.

The detector is paired with a new X-ray tube design, featuring reduced focal spot sizes, as small 0.4 mm × 0.5 mm and rotating at 10,800 rpm to efficiently dissipate heat. Building on Aquilion Precision's hardware advancements, next generation AIDR*1 3D, a fast hybrid reconstruction algorithm, and FIRST*2, a fully-iterative reconstruction algorithm, have both been optimized specifically for Precision. The algorithms offer powerful tools for maximizing spatial resolution while reducing noise and radiation dose usage.

In order to better understand the capabilities of the Aquilion Precision and each of its modes (Table 1), the spatial resolution, noise, and low contrast detectability performance evaluations for these modes will be explored in detail.

Spatial resolution

The Aquilion Precision utilizes detector elements half the size of previous systems in both the in-plane and longitudinal directions, leading to ultra-sharp image detail. In order to analyze in-plane spatial resolution performance from a quantitative, physics-based point of view the modulation transfer function (MTF) is used. The MTF plots the percent contrast preserved for each degree of detail, expressed in increments of frequency (lp/cm): perfect preservation of low frequency (low detail) information in an image would be represented by an MTF value of 1, while partial preservation of high frequency (high detail)information would be represented by a value less than unity (eg, 50% preservation would yield an MTF value of 0.5).

The MTF is often quoted by giving the MTF value associated with the 2% value of the plot as the "cutoff" frequency. As can be seen in Figure 4, the 2% MTF on Precision for a high resolution kernel doubles in going from NR mode to HR mode, to an astonishing 46.1 lp/cm.

In routine scanning, such as a typical adult protocol, the tremendous increase in spatial resolution is demonstrated in the MTFs in Figure 5. Notice the use of FIRST with HR mode results in even greater spatial resolution for routine protocols.

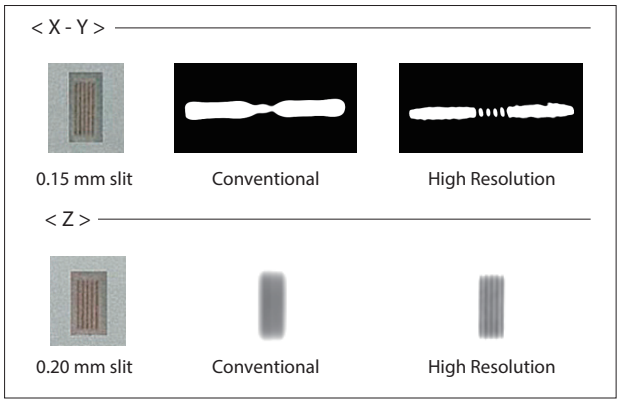

Figure 2 Slit phantoms demonstrating 150 µm in-plane resolution and 200 µm longitudinal resolution.

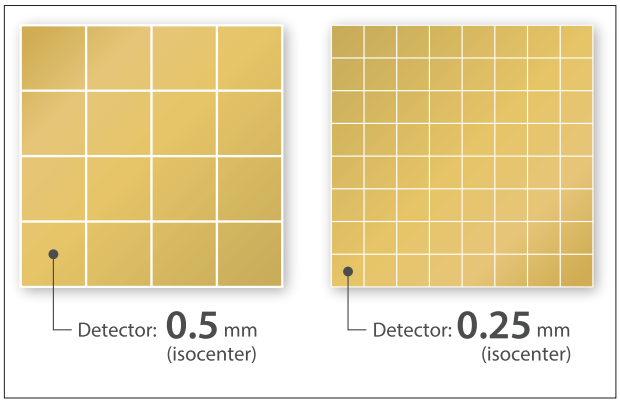

Figure 3 The Aquilion Precision features detector elements and septa half the size of their predecessor.

*1 Adaptive Iterative Dose Reduction, *2 Forward projected model-based Iterative Reconstruction SoluTion

In terms of longitudinal spatial resolution, the Slice Sensitivity Profile (SSP) is used to quantify the spread of the nominal slice thickness along the z-axis of the patient (Figure 6). The narrower the SSP, the more the z-axis resolution is preserved, the less partial volume averaging in-plane, and the sharper the MPRs.

Contrast-to-noise ratio (CNR) and noise

The Contrast-to-Noise Ratio (CNRs) is a measure of image quality that, in one of its simplest forms, is determined by taking the absolute value of the difference in mean CT number of an object from its background and dividing it by the standard deviation of noise (SD) of the background.

$$\mathbf{CNR= \Delta Mean\ CT/SD}$$

This expression for CNR is useful for image quality comparisons when sources of spatial resolution variation, as well as signal and noise texture variation, are held constant. However, when spatial resolution, signal power and/or noise texture vary significantly, this CNR metric is too simple to be an accurate measure of image quality. For example, note that in the two images in Figure 1, both images have similar image quality and low contrast detectability, yet very different CNR values. Both images are reconstructed with the same kernel and AIDR 3D reconstruction settings, but the image on the right is a 1024 × 1024 image generated with the Aquilion Precision's HR mode and the image on the left is a 512 × 512 image generated in NR mode.

Table 1 The Aquilion Precision offers the user three modes, depending on the desired level of image quality.

Preset	Collimation	Detector Channels	Reconstruction Matrix	Detector Binning
Super High Resolution	0.25 mm × 160	1792 Ch	1024	
High Resolution	0.5 mm × 80	1792 Ch	1024	
Normal Resolution	0.5 mm × 80	896 Ch	0512	

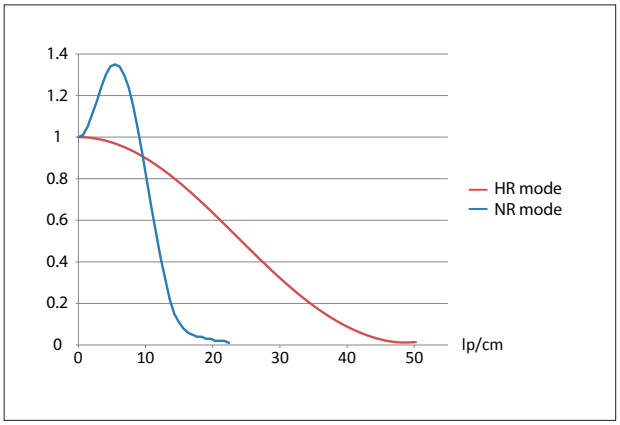

Figure 4 The 2% MTF value reaches 46.1 lp/cm on the Aquilion Precision in HR mode.

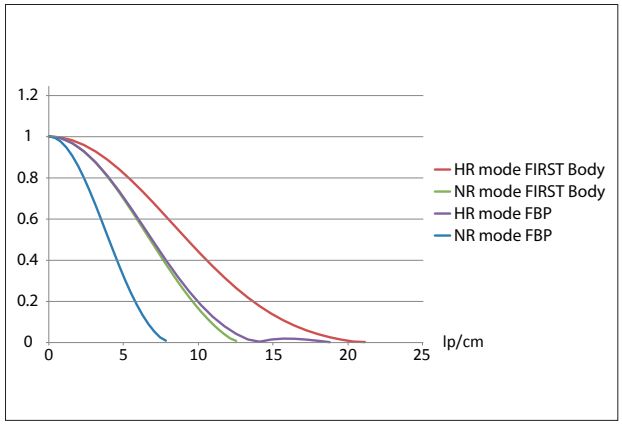

Figure 5 Aquilion Precision MTFs for typical Body protocols in NR and HR mode.

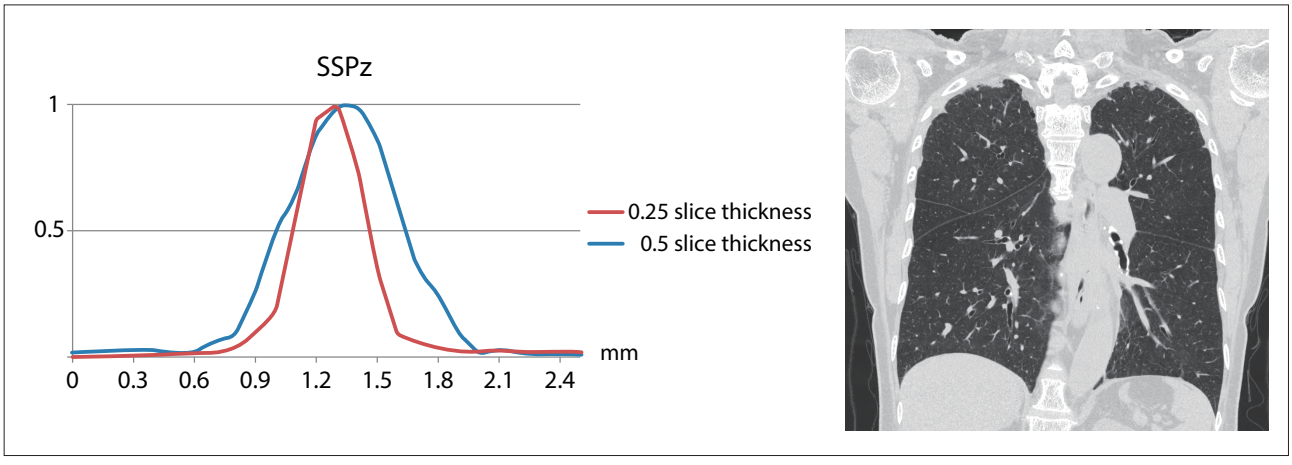

Figure 6 The Aquilion Precision SHR mode uses 0.25 mm acquisition slice thickness.

The reason the CNR metric is misleading as an image quality metric in this illustration is threefold.

1) Spatial resolution

Improved object sharpness plays a role in improved detectability.

2) Signal power

The power of a signal is defined as the sum of the square of the pixel intensity over the region of interest. In fact, many common measures of SNR and CNR use signal power in the numerator.

$$\mathrm{SNR} = \frac{\sum_{x=0}^{M-1}\sum_{y=0}^{N-1}\hat{f}(x,y)^2}{\sum_{x=0}^{M-1}\sum_{y=0}^{N-1}\left[f(x,y) - \hat{f}(x,y)\right]^2}$$

Equation 1 Signal-to-noise ratio formula.

When the mean value alone is substituted for the numerator, information about the signal power relative to the noise can get lost. For example, in the NR mode, 512 × 512 image of the Gammex ACR phantom the 6 HU-contrast cylinder that is 25 mm in diameter is more detectable than the 6 HU-contrast cylinders that are only 6 mm in diameter; yet a simple CNR — as defined by the mean ΔHU over the standard deviation — would suggest they are equally detectable.

Similarly, the signal power of an object of a given size and HU value acquired in HR mode and presented with a 1024 matrix will have four times the power of the same object acquired in HR mode. This increase is signal power helps balance the increase in noise discussed in the next section. This effect is reflected in more sophisticated measures of image quality, as will be discussed later.

2a) Noise properties-magnitude

The magnitude of noise is generally quantified by the standard deviation (SD) of noise or its square, the variance of noise. When comparing a 1024 reconstruction matrix, for example, to a standard 512 reconstruction matrix for a given size field of view, the pixel size of the 1024 matrix will be one quarter that of the 512 matrix. This reduction in pixel size in turn reduces the number of photons per pixel, increasing the standard deviation by a factor of two (or variance by a factor of four) at a given radiation dose when old-fashioned, linear Filtered Backprojection (FBP) reconstruction is applied. However, with iterative reconstruction the relationship between standard deviation and pixel size is more complex.

As can be seen in the Table 2, the standard deviation at the same radiation dose increases by over by 2x with FBP in HR and SHR mode, compared to NR mode, for the same slice thickness. However, with FIRST, the fully-iterative reconstruction optimized specifically for the Aquilion Precision, the standard deviation in HR and SHR mode is very similar to the current clinical standard of AIDR 3D with NR mode acquisition and reconstruction.

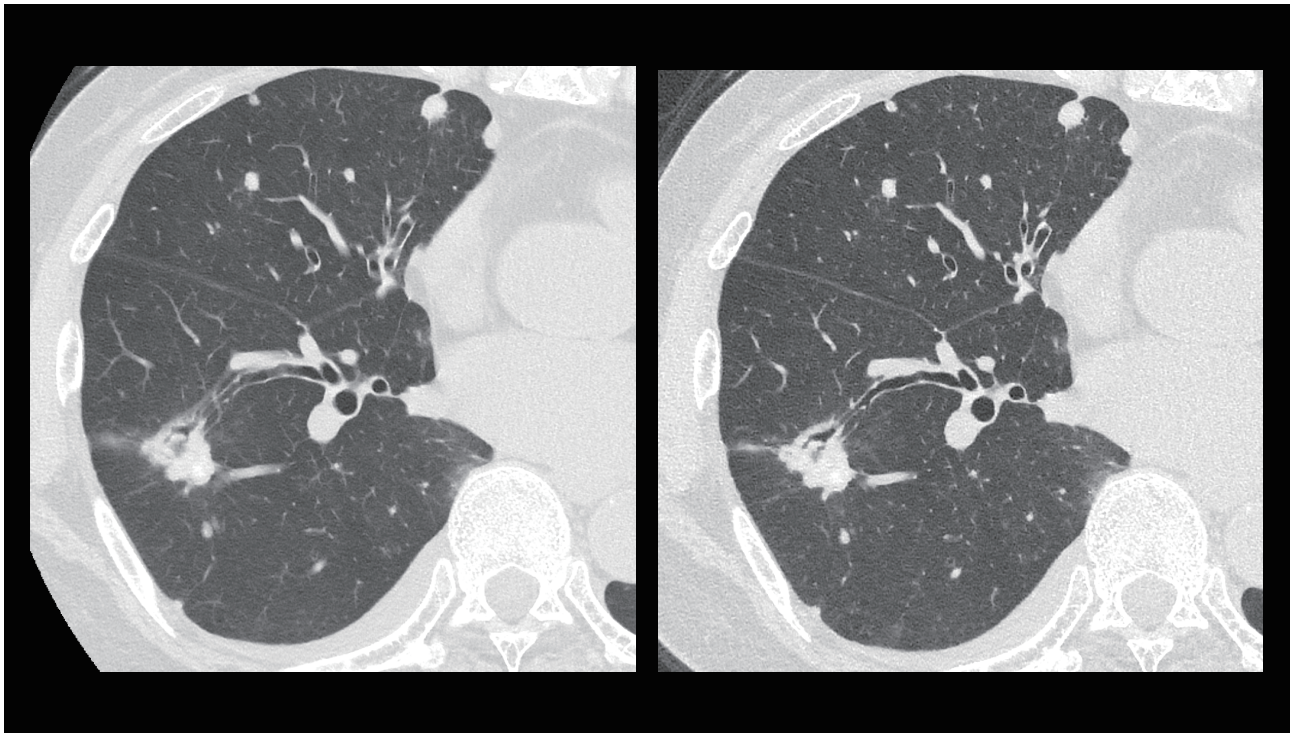

Figure 7 This SHR mode (on the right) lung scan reveals greater anatomical and nodule detail than conventional resolution imaging (on the left).

Table 2 Standard deviation of noise values in NR, HR, and SHR modes with FBP, AIDR, and FIRST.

	NR	HR	SHR
FBP	24.9 HU	61.5 HU	65.2 HU
AIDR	14.4 HU	21.7 HU	23.4 HU
FIRST	8.2 HU	14.2 HU	14.5 HU

2b) Noise properties-noise texture

While the calculation of the standard deviation of noise for any size matrix is straightforward, the SD value is not a reliable measurement of image quality,[1] in part because noise magnitude is only one aspect of noise. The texture of the noise can greatly impact how that noise affects detectability. For example, in Figure 8, there are two 512 images with the same standard deviation of noise, but different object detectability, demonstrating that texture, or noise appearance, is an important aspect of image quality.

The main method to characterize noise texture is the Noise Power Spectrum (NPS). Much like the MTF, the NPS expresses noise in terms of spatial frequency (lp/cm) content. In fact, the NPS quantifies the variance of noise at each spatial frequency: noise with high variance in the low frequencies tends to appear chunky or thick-grained (such as the image on the left in Figure 8), while noise with high variance in the high frequencies tends to appear fine-gained (such as the image on the right in Figure 8). The objects in the higher frequency noise are easier to detect in part because most signals are primarily low frequency in nature.

With a 1024 × 1024 or greater matrix size, higher spatial frequencies are realized in the image, leading to the introduction of higher frequency signal and noise than is possible with a 512 × 512 matrix.

As can be seen in Figure 9, the noise texture in HR mode and NR mode is similar in the low frequencies but overall much higher frequency in nature with HR reconstruction. How do these differences in noise appearance impact detectability? To discover that, we need use an even more sophisticated measure of image, the low contrast detectability observer study.

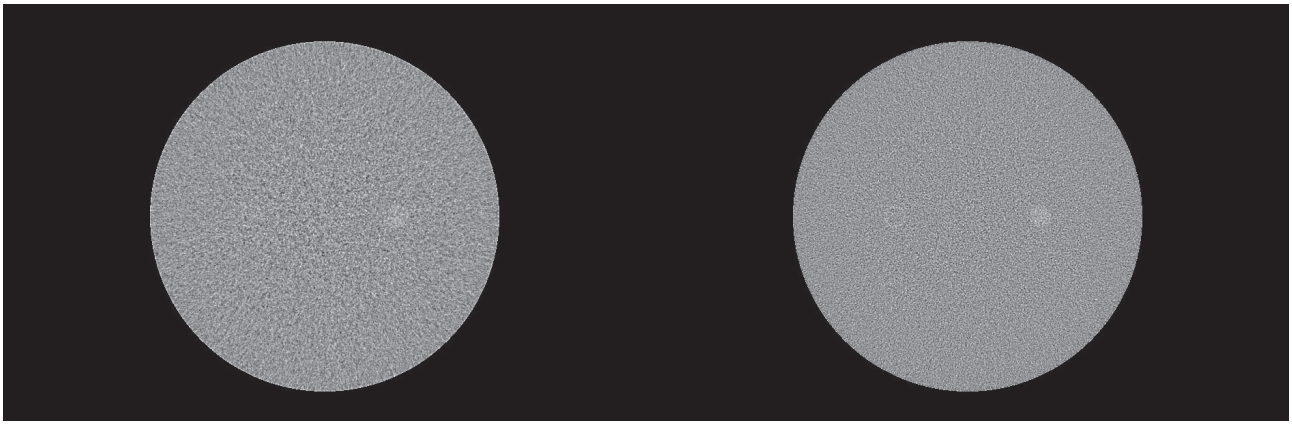

Figure 8 These two images have the same standard deviation of noise but different noise texture. The test objects are more easily detectable in the high frequency noise texture on the right, illustrating the importance of noise texture in assessing image quality.

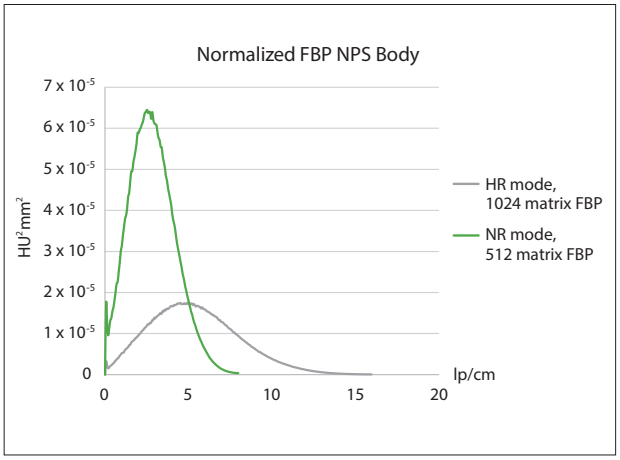

Figure 9 Normalized noise power spectra in NR and HR mode

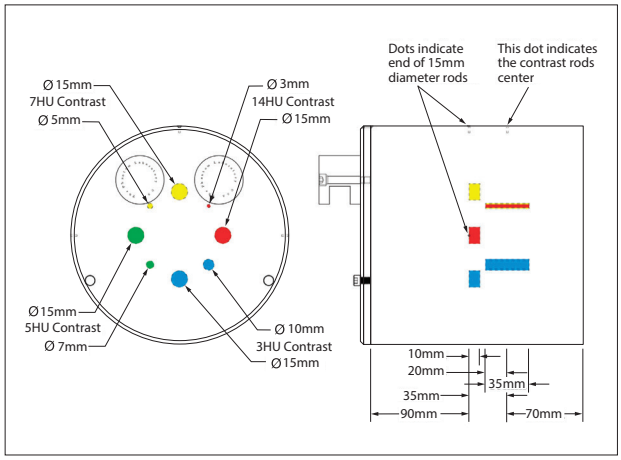

Figure 10 Schematic image of MITA CCT189 Low Contrast Body Phantom

Low contrast detectability and dose

Conventional image quality metrics offer only a piece of the overall image quality picture and, individually, do not always provide a reliable characterization of overall low contrast object detectability. This is particularly true for the Aquilion Precision with high resolution, 1792 detector channel acquisition and 1024/2048 matrix reconstruction. The task-based model observer provides a pragmatic paradigm for objective assessment of image quality, taking the various components of image quality into account, by modelling an observer's ability to detect a low contrast object.

Model observers have a long history in the literature of tracking with human observer performance on low contrast detectability tasks, including the Non Prewhitening Matched Filter Model Observer (NPW).[2-14] In collaboration with the FDA, industry manufacturers developed a standardized low contrast detectability (LCD) phantom specifically for use in observer studies used to evaluate product LCD performance.

A typical model observer experimental setup operates by analyzing hundreds of pairs of image ROIs, one with the low contrast signal present and one with the low contrast signal absent. The output of the model observer can be the Area Under the Curve (AUC) value and/or its transform the detectability index (d'). For this experimental setup, the AUC can be thought of as the percent of ROIs correctly identified as having the signal present or absent; the d' is a corresponding, sophisticated signal-to-noise value that can be expressed as the following:

$$(d'_{NPW})^2 = \frac{\left[\iint MTF^2(u,v)W^2_{Task}(u,v)dudv\right]^2}{\iint NPS(u,v)MTF^2(u,v)W^2_{Task}(u,v)dudv}$$

Equation 2

Where W represents the low contrast signal (rod) of interest and the MTF and NPS, as previously described, for the relevant scan conditions.

As can been from Equation 2, the d' ties together the signal, spatial resolution, and noise properties into a single, quantified LCD value at a particular dose. The higher the d' (or AUC) the better the low contrast detectability of an object.

In order to compare LCD and dose on the Aquilion Precision, the average AUC of several low contrast rods were measured at a typical clinical dose in NR mode, using FBP, AIDR, and FIRST reconstruction, and then in HR mode and SHR mode. Several additional dose levels were acquired for HR and SHR.

Table 3 Average AUC for Body conditions

Scan Mode	CTDI (mGy)	FBP	AIDR 3D	FIRST
NR	**15.9**	**0.891**	**0.918**	**0.939**
HR	15.9	0.873	0.915	0.934
	18.2	0.887	0.934	0.939
	20	0.901	0.93	0.944
	22.3	0.907	0.936	0.951
SHR	15.9	0.881	0.915	0.93
	18.2	0.89	0.92	0.936
	20	0.891	0.931	0.939
	22.3	0.907	0.94	0.949

Table 4 Average AUC for Head conditions

Scan Mode	CTDI (mGy)	FBP	AIDR 3D	FIRST
NR	58.5	0.901	0.909	0.912
HR	58.5	0.891	0.918	0.924
	69.5	0.907	0.928	0.932

As shown in Table 3 and 4, LCD equivalent to an NR mode baseline is achieved for HR and/or SHR mode with either no dose increase or a modest dose increase, well within ACR-AAPM DRLs.

Conclusion

The Aquilion Precision offers a new experience in image detail, which may help the clinician more accurately describe pathology. Quantitative analysis of image quality is key to understanding the Aquilion Precision's advanced technology, appropriately relating its properties to conventional normal resolution imaging, and benchmarking its superior performance capabilities. It is vital to use caution when using simple metrics, such as standard deviation and CNR values, when evaluating system performance. Sophisticated metrics, such as the model observer-based LCD evaluation better quantify the relationship between image quality and dose. With equivalent LCD at standard radiation doses and the power of ultra-high spatial resolution, the Aquilion Precision is the next step in the evolution of CT.

References:

1. Vaishnav et al., Objective assessment of image quality and dose reduction in CT iterative reconstruction, *Med. Phys*., 2014.
2. W. J. H. Veldkamp, M. A. O. Thijssen, and N. Karssemeijer, "The value of scatter removal by a grid in full field digital mammography," *Medical Physics*, vol. 30, pp. 1712–1718, 2003.
3. ICRU Report 54. "Medical Imaging — The Assessment of Image Quality, International Commission on Radiation Units and Measurements," Bethesda,MD, 1996
4. Beutel J., Kundel H., and Van Metter R., Handbook of medical imaging: Physics and psychophysics (SPIE, Bellingham, WA, 2000).
5. Richard S. and Siewerdsen J. H., "Comparison of model and human observer performance for detection and discrimination tasks using dual-energy X-ray images," *Medical Physics*, vol. 35, pp. 5043–5053, 2008.
6. Yu L., Leng S., Chen L., Kofler J. M., Carter R. E., and McCollough C. H., "Prediction of human observer performance in a 2-alternative forced choice low-contrast detection task using channelized Hotelling observer: Impact of radiation dose and reconstruction algorithms," *Medical Physics*, vol. 40, 2013.
7. Leng S, Yu L, Zhang Y, Carter R, Toledano AY, McCollough CH, "Correlation between model observer and human observer performance in CT imaging when lesion location is uncertain," *Medical Physics*, vol. 40(8), 2013.
8. A. E. Burgess, "Statistically defined backgrounds: performance of a modified nonprewhitening observer model," *J Opt Soc Am A Opt Image Sci Vis*, vol. 11, pp. 1237-42, Apr 1994.
9. J. A. Segui and W. Zhao, "Amorphous selenium flat panel detectors for digital mammography: Validation of a NPWE model observer with CDMAM observer performance experiments," *Medical Physics*, vol. 33, pp. 3711-3722, 2006.
10. Y. Zhang, B. T. Pham, and M. P. Eckstein, "Automated optimization of JPEG 2000 encoder options based on model observer performance for detecting variable signals in X-ray coronary angiograms," *IEEE Trans Med Imaging*, vol. 23, pp. 459-74, Apr 2004.
11. P. Monnin, F. Bochud, and F. Verdun, "Using a NPWE model observer to assess suitable image quality for a digital mammography quality assurance programme," *Radiation Protection Dosimetry*, p. ncq010, 2010.
12. I. Hernandez-Giron, J. Geleijns, A. Calzado, and W. Veldkamp, "Automated assessment of low contrast sensitivity for CT systems using a model observer," *Medical Physics*, vol. 38, pp. S25-S35, 2011.
13. DeLong ER1, DeLong DM, Clarke-Pearson DL. "Comparing the areas under two or more correlated receiver operating characteristic curves: a nonparametric approach" *Biometrics*, vol. 44(3), 1988.
14. Myers, KJ, Barrett, MC, Borgstrom, MC, Patton DD, and Seely GW. "Effect of noise correlation on detectability of disk signals in medical imaging," *Journal of Optical Society of America*, Vol.2(10), 1985.

CANON MEDICAL SYSTEMS CORPORATION
https://global.medical.canon

Model number:TSX-304A MCACT0321EAB 2018-06 CMSC/CPL/Printed in Japan

Canon Medical Systems Corporation meets internationally recognized standards for Quality Management System ISO 9001, ISO 13485.
Canon Medical Systems Corporation meets the Environmental Management System standard ISO 14001.

The following document was created prior to the name change and therefore reflects our former company name.

Made For life